ADVANCED OPTICAL MATERIALS

Supporting Information

for *Adv. Optical Mater.*, DOI 10.1002/adom.202301912

Vibrational Coupling to Quasi-Bound States in the Continuum under Tailored Coupling Conditions

Keisuke Watanabe, Hemam Rachna Devi, Masanobu Iwanaga and Tadaaki Nagao*

Supporting Information

Vibrational Coupling to Quasi-Bound States in the Continuum under Tailored Coupling Conditions

Keisuke Watanabe, Hemam Rachna Devi, Masanobu Iwanaga, and Tadaaki Nagao*

S1. *Q* factors considering material absorptions

In the main text, the Q factors were calculated with the extinction coefficient k set to zero to separate Q_r and Q_{nr}. Here, we calculate Q factors considering the material absorptions of Si and SiO_2, whose dielectric functions were taken from Palik.[41] As shown in Figure S1, the calculated Q factors with and without material absorption exhibit similar trends with a slight difference. Because the total Q factors with $k \neq 0$ are expressed as $Q_{tot}^{-1} = Q_R^{-1} + Q_{abs}^{-1}$, the Q_{abs} is estimated to be approximately 900 in this wavelength range.

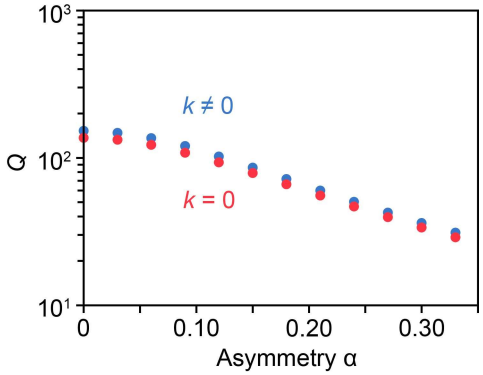

Figure S1. Comparison of the FDTD calculated Q factors with and without consideration of material absorption.

S2. Comparison of FDTD simulated and experimental spectra

As shown in Figure. S2, the simulation and experiment show good agreement for both the qBIC and coupled qBIC-PMMA resonances. The slight differences in both resonances indicate that the resonance peaks were slightly blueshifted in the experiment. This can be attributed to

structural deformations (e.g., rounded corners) by fabrication errors. For coupled qBIC-PMMA resonances, the triple peaks are pronounced in the simulation, especially when α is small. An intuitive explanation for this is that the absorption of the intrinsic uncoupled PMMA molecules is unexpectedly large, presumably because of the less accurate dielectric constants of PMMA.

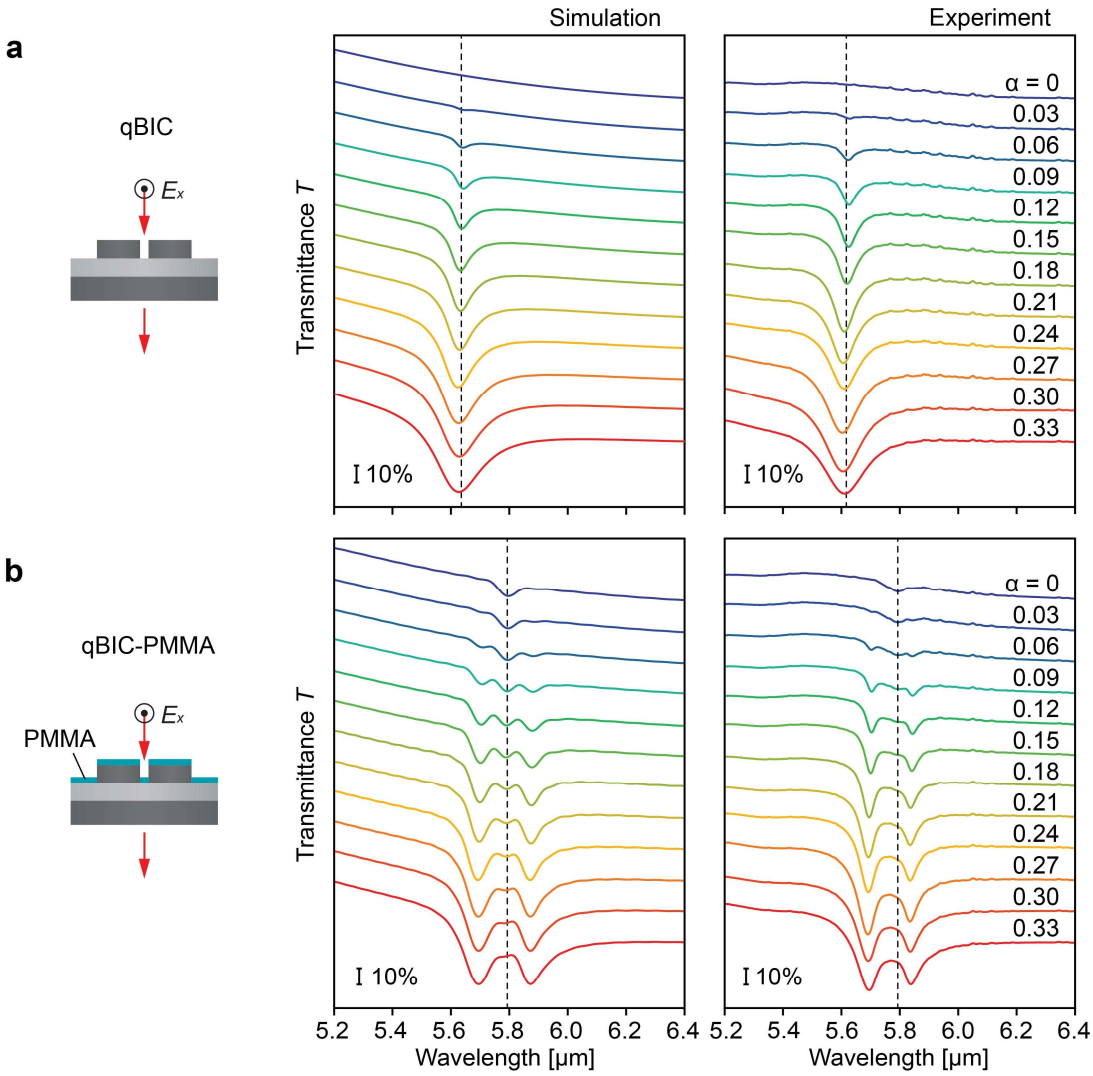

Figure S2. Transmission spectra of (a) bare and (b) PMMA-coated silicon metasurfaces with different α. The schematic shows a metasurface excited by vertically incident *x*-polarized light. The dashed lines indicate the approximate peak positions of the qBIC modes for (a) and the C=O modes for (b). For clarity, the spectra are shifted vertically.

S3. Temporal coupled mode theory for asymmetric metasurfaces coupled with molecules

Temporal coupled mode theory (TCMT) offers a means of describing the resonance behaviors of a coupled cavity-molecular system as well as its enhanced molecular signal. In the following section, we derive a theoretical model for metasurfaces with asymmetric cladding layers

coupled to molecules on the top surface. As illustrated in Figure 4a in the main text, we consider a coupled cavity-molecular system with two input ports: the input traveling wave $s_+ = [s_{1+}\ s_{2+}]^T$ and the output traveling wave $s_- = [s_{1-}\ s_{2-}]^T$. The coupled-mode equations are as follows:

$$\frac{d}{dt}A = i\omega_c A - \left(\frac{1}{\tau_1}+\frac{1}{\tau_2}+\frac{1}{\tau_{nr}}\right)A + Ds_+ + igM, \tag{S1}$$

$$\frac{d}{dt}M = i\omega_m M - \frac{1}{\tau_m}M + igA, \tag{S2}$$

$$s_- = Cs_+ + D^T A. \tag{S3}$$

where A and M are the field amplitudes of the qBIC and vibrational modes, whose resonance frequencies are ω_c and ω_m, respectively. The coupled cavity-molecular system has a coupling strength g, and the coupled system couples outside the medium with an upward radiative rate τ_1^{-1} and a downward radiative rate τ_2^{-1}. τ_{nr}^{-1} is the nonradiave decay rate caused by the absorption of the materials and scattering losses due to fabrication errors. C is the scattering matrix for transmission and reflection without the resonances given by $C = e^{i\phi}\begin{pmatrix} r & it \\ it & r \end{pmatrix}$, where r and t are the reflection and transmission coefficients, respectively, that account for the Fano lineshape of the resonance caused by the interference between the broad background spectrum and the sharp cavity mode. φ is the phase factor, which depends on the reference plane position and is set to zero. D is the coupling coefficient between the two ports and is given by $D = (d_1\ d_2)$. Assuming that the resonance amplitudes A and M have time dependence $e^{-i\omega t}$ and $s_{2+} = 0$ (only one input port from the top), solving Equation (S1)−(S3) gives an expression for the reflection spectrum of the transverse electric (TE)-like mode as follows:

$$R = \left|\frac{s_{1-}}{s_{1+}}\right|^2 = \left| r - \frac{2e^{i2\theta_1}/\tau_1}{i(\omega-\omega_c)+\frac{1}{\tau_1}+\frac{1}{\tau_2}+\frac{1}{\tau_{nr}}+\frac{g^2}{i(\omega-\omega_m)+1/\tau_m}}\right|^2$$

$$= \left| r - \frac{2(\cos 2\theta + i\sin 2\theta)/\tau_1}{i(\omega-\omega_c)+\frac{1}{\tau_1}+\frac{1}{\tau_2}+\frac{1}{\tau_{nr}}+\frac{g^2}{i(\omega-\omega_m)+1/\tau_m}}\right|^2. \tag{S4}$$

As mentioned in the main text, this equation does not consider the interactions between the molecules and the input port for simplicity (there is an interaction only between the cavity and molecules). Here, we assume $d_1 = \sqrt{\frac{2}{\tau_1}}e^{i\theta_1}$ and $d_2 = \sqrt{\frac{2}{\tau_2}}e^{i\theta_2}$ by defining the respective phases θ_1

and θ_2. From the energy conservation and time-reversal symmetry, C and D satisfy $d_1^* d_1 = 2/\tau_1$, $d_2^* d_2 = 2/\tau_2$, and $C\begin{pmatrix} d_1 \\ d_2 \end{pmatrix}^* = -\begin{pmatrix} d_1 \\ d_2 \end{pmatrix}$. By solving these equations, we obtain:

$$\cos 2\theta = \frac{\tau_1}{2r}\left(-\frac{r^2}{\tau} - \frac{1}{\sigma}\right), \tag{S5}$$

$$\sin 2\theta = \pm\frac{\tau_1}{2r}\sqrt{\frac{4r^2}{\tau_1^2} - \frac{r^4}{\tau^2} - \frac{1}{\sigma^2} - \frac{2r^2}{\tau\sigma}}, \tag{S6}$$

where

$$\frac{1}{\tau} = \frac{1}{\tau_1} + \frac{1}{\tau_2}, \tag{S7}$$

$$\frac{1}{\sigma} = \frac{1}{\tau_1} - \frac{1}{\tau_2}. \tag{S8}$$

The transmission spectra $T = 1 - R$ can be obtained by substituting Equation (S5)-(S8) into (S4). As previously pointed out,[35,36] there is a fundamental bound on τ_1/τ_2 constrained by $(1 + r)/(1 - r)$. For the model fitting of the experimental data and calculation of the enhanced molecular signal, we also considered this constraint and used the FDTD-calculated Q_{top} and Q_{bottom}.

S4. Effect of BOX layer thickness on resonance spectra

The presence of the BOX layer in an SOI wafer causes interference between the top silicon metasurface and bottom silicon substrate. The resulting Fabry–Pérot background sometimes hinders the weak qBIC and vibrational modes. Therefore, the BOX layer thickness should be carefully designed depending on the resonance wavelength to be measured. Figure S3 shows the transmission spectra of metasurfaces with different BOX layer thicknesses. When $\alpha = 0.1$, the qBIC mode of interest appears, and the resonance dip becomes apparent when the background spectrum is close to 1, that is, when the BOX layer thickness is approximately 2500 nm. Nevertheless, the 2000-nm BOX layer in our work still provides a sharp resonance dip, providing a means for measuring the resonance modes.

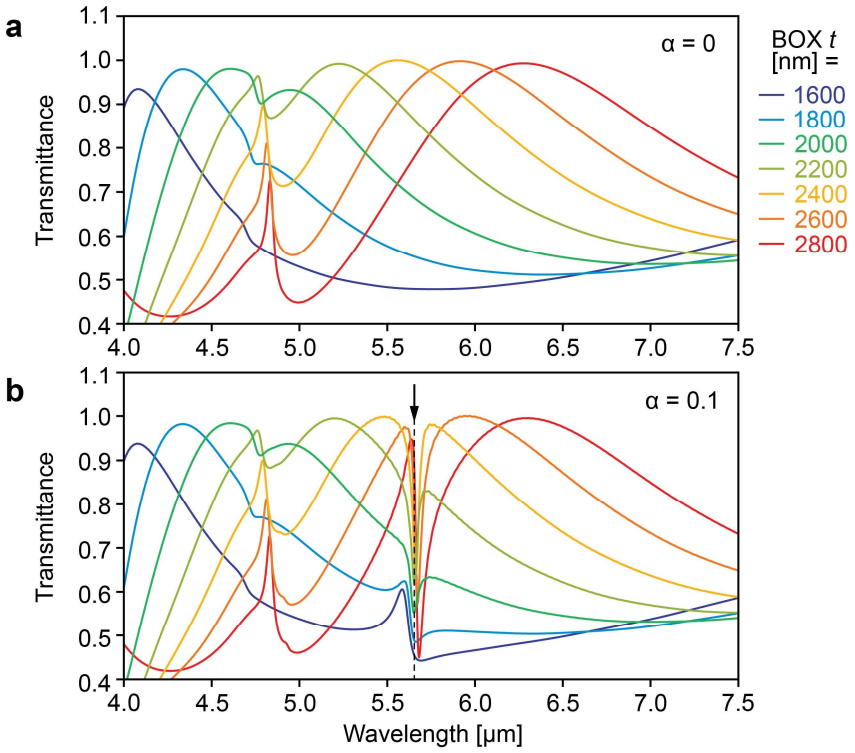

Figure S3. Transmission spectra of the metasurfaces with different BOX layer thicknesses when (a) α = 0 and (b) α = 0.1. The arrow indicates the wavelength at which the qBIC mode appears.